Organic Electronics 49 (2017) 406–414

Contents lists available at ScienceDirect

Organic Electronics

journal homepage: www.elsevier.com/locate/orgel

An aromatic amine-containing polymer as an additive to ambipolar polymer semiconductor realizing unipolar n-type charge transport

Yinghui He [a], Jesse T.E. Quinn [a], Suhyun Lee [a], Guan Ying Wang [a], Xu Li [b], Jinliang Wang [b], Yuning Li [a, *]

[a] Department of Chemical Engineering and Waterloo Institute for Nanotechnology (WIN), 200 University Ave W, Waterloo, Ontario, N2L 3G1, Canada
[b] Institute of Chemistry, Henan Academy of Sciences, 56 Hongzhuan Road, Jinshui District, Zhengzhou, Henan, 450002, China

ARTICLE INFO

Article history:
Received 17 April 2017
Received in revised form
20 June 2017
Accepted 10 July 2017
Available online 11 July 2017

Keywords:
Amine-containing polymer
Ambipolar polymer
Unipolar n-type OTFTs
Low off current
Hole trapping

ABSTRACT

We report the synthesis of an aromatic amine-containing polymer (**PDPAT-12**) and the use of this polymer as an effective additive to an ambipolar polymer semiconductor (**PIBDFBT-e37**) to realize unipolar n-type charge transport in organic thin film transistors (OTFTs). With 10 wt% **PDPAT-12** addition to **PIBDFBT-e37**, the OTFTs achieved unipolar n-type charge transport with electron mobility of up to 0.42 $cm^2 V^{-1} s^{-1}$ in nitrogen and 0.19 $cm^2 V^{-1} s^{-1}$ in air. Moreover, the polymer blend demonstrated improved stability towards ambient air (retaining 50% of its initial electron mobility after exposed in air for 28 days) than the pristine **PIBDFBT-e37** (retaining 13% of its initial electron mobility under the same conditions) and the **PIBDFBT-e37**:PEI (polyethylenimine) blend, which lost transistor behaviour almost instantly once exposed to ambient air. Our results show that the use of this aromatic amine-containing polymer as an additive can convert an ambipolar polymer into an n-type unipolar polymer in OTFTs with much improved air stability.

1. Introduction

π-Conjugated polymers are used as semiconducting materials in organic electronics because of their flexibility, mechanical robustness, solution processability and potential of low cost production [1–3]. In recent years, donor-acceptor (D-A) π-conjugated polymers that incorporate alternating electron donor and acceptor units in their backbones have been of particular interest as channel materials for organic thin film transistors (OTFTs) owing to the shortened chain-to-chain π-π distance due to the strengthened intermolecular interaction. High performance OTFTs with field-effect mobility over 5 $cm^2 V^{-1} s^{-1}$ have been realized using D-A polymers [4–8], which opens up opportunities to a wide variety of electronic applications, e.g., flexible display backplanes and radio-frequency identification tags [9]. On the other hand, due to the orbital hybridization, D-A polymers generally have rather small band gaps with deepened lowest unoccupied molecular orbital (LUMO) energy levels and elevated highest occupied molecular orbital (HOMO) energy levels, which favours charge injection and transport for electrons and holes, respectively. Thus, ambipolar charge transport characteristics are often observed for D-A polymers in OTFTs [10–16]. Although using ambipolar polymer semiconductors can simplify the fabrication of complementary metal oxide semiconductor (CMOS)-like logic circuits with a single-component ambipolar semiconductor, the inevitable large standby currents of such ambipolar OTFT-based logic circuits can lead to high power consumption and low on/off current ratios [17,18]. Therefore, unipolar p-type and n-type OTFTs are preferred for CMOS-like logic circuit fabrication in view of device performance. While quite a number of D-A polymers have demonstrated unipolar p-type charge transport with high field-effect mobility [5,7,19–22], much fewer unipolar n-type D-A polymer semiconductors have been reported so far [23–25]. Previously, our group and several other groups reported a strong electron acceptor building block, (3*E*,7*E*)-3,7-bis(2-oxoindolin-3-ylidene)benzo[1,2-*b*:4,5-*b*′]difuran-2,6(3*H*,7*H*)-dione (IBDF) for constructing D-A polymers for OTFTs [11,13]. IBDF-based polymers generally exhibited excellent electron charge transport characteristics [26–29] and recently a fluorinated IBDF-based polymer demonstrated an extremely high electron mobility of 14.9 $cm^2 V^{-1} s^{-1}$ in a top-gate bottom-contact OTFT device [30]. However, quite a few IBDF-based D–A polymers were found to show ambipolar charge transport

* Corresponding author.
E-mail address: yuning.li@uwaterloo.ca (Y. Li).

http://dx.doi.org/10.1016/j.orgel.2017.07.016
1566-1199/

characteristics [11,13,31–33], which is suboptimal for the CMOS-like logic circuits. We recently reported a strategy based on the use of polyethylenimine (PEI) as an additive to ambipolar and p-type polymer semiconductors that converts these polymers into unipolar n-type semiconductors [34]. Our study showed that PEI could raise the Fermi energy of the polymer blend to fill the electron traps and that the nitrogen lone pairs in PEI can act as hole traps and therefore suppress hole transport.

In this work, we first succeeded in using PEI to convert a previously reported ambipolar IBDF-based polymer, **PIBDFBT-e37** (Fig. 1) into an n-type polymer for use in bottom-gate bottom-contact (BGBC) OTFTs. However, in ambient air the OTFT devices showed seriously degraded transistor characteristics and suffered from high off-current, which seemed to be caused by the moisture enhanced n-doping effect of the highly hygroscopic PEI. To overcome the moisture sensitivity issue of using PEI, we designed a new aromatic amine-containing polymer (**PDPAT-12**, Fig. 1), which is much more hydrophobic than PEI. We found that with 10 wt% **PDPAT-12** addition, the hole transport of **PIBDFBT-e37** in BGBC OTFTs was completely suppressed and the OTFTs exhibited unipolar n-type charge transport with high average electron mobility of 0.42 $cm^2\ V^{-1}\ s^{-1}$ in nitrogen and 0.19 $cm^2\ V^{-1}\ s^{-1}$ in air.

2. Results and discussion

Pristine **PIBDFBT-e37** was tested as a channel semiconductor in BGBC OTFTs, which showed typical ambipolar charge transport performance with more pronounced electron transport (Table 1). The highest electron mobility of 0.29 $cm^2\ V^{-1}\ s^{-1}$ was achieved when the polymer film was annealed at 150 °C, while the highest hole mobility of 0.077 $cm^2\ V^{-1}\ s^{-1}$ was obtained at an annealing temperature of 200 °C. The on/off current ratios are quite low, ca. 10^3 for n-type operation and ca. 10^2 for p-type operation. Low on/off current ratios are typical for OTFTs using ambipolar semiconductors [6,15,16,35]. To convert the ambipolar **PIBDFBT-e37** into n-type polymer by suppressing the hole transport characteristics, PEI (Fig. 1) was used as an additive to **PIBDFBT-e37** because this amine polymer was found to be very effective for the n-unipolarization of a number of ambipolar and p-type polymers [34]. The amount of PEI in the **PIBDFBT-e37**: PEI blend was kept at 2 wt%, which was found to be optimal for realizing unipolar electron transport while enhancing or maintaining the electron transport performance [34]. When the devices were tested under nitrogen (oxygen and H_2O levels below 1 ppm), unipolar n-type charge transport characteristics were observed for devices annealed at all temperatures tested (100, 150 and 200 °C). The highest average electron mobility of 0.28 $cm^2\ V^{-1}\ s^{-1}$ was achieved for the device annealed at 150 °C (Fig. 2a). When the devices were tested in ambient air (with a relative humidity (RH) of 50%), they all suffered from a high off-current (ca. 10^{-5} A versus ca. 10^{-7} A measured in the glove box) with low mobilities of ~10^{-3} $cm^2\ V^{-1}\ s^{-1}$ (Fig. 2b). To investigate the cause for the unusual high conductivity of the channel layer and thus high off-current in ambient air, we first fabricated the OTFT devices using the pristine **PIBDFBT-e37** as the channel material and tested them following the same procedure used for the polymer blends. Both the devices tested in the glove box and in ambient air had similar off-current (~10^{-7} A). This suggests that the increase in the off-current does not originate from the interaction of **PIBDFBT-e37** with some component(s) in ambient air. Next, we deposited a PEI film on the same substrate and measured the diode I-V characteristics (at a gate voltage of 0 V) in dry nitrogen and ambient air, respectively (Fig. S1). The current measured in dry nitrogen is ~2–3 × 10^{-9} A while the current measured in ambient air is only slightly higher at ~3–4 × 10^{-9} A. These results clearly indicate that PEI alone is not responsible for the increased off-current observed in the OTFT devices using the blend films in ambient air. Instead, the combination of **PIBDFBT-e37** and PEI must interact with oxygen or moisture present in ambient air to induce an increase in the electrical conductivity, or doping, of the blend films [36]. To further identify which of the two species has the greater effect on the doping of the polymer blends, we tested the OTFT devices using the polymer blends in dry air and moist nitrogen. The devices tested in dry air exhibited similar n-type transistor characteristics with off current (~10^{-8} A, Fig. 2c) comparable to devices tested in dry nitrogen (~10^{-7} A). On the other hand, the OTFTs tested in moist nitrogen showed a serious degradation in transistor performance as well as a large increase in the off-current to ~10^{-5} A, which is similar to the value observed for the OTFTs tested in ambient air (Fig. 2d). The results unambiguously prove that moisture is primarily responsible for the doping of the **PIBDFBT-e37**:PEI blend in ambient air. Since PEI is highly hygroscopic and basic (pKa value between 8.2 and 9.9) [37], it can absorb the moisture in ambient air to release OH^-, which may n-dope **PIBDFBT-e37** and lead to a significant increase in conductivity. Previous studies indeed have shown that hydroxides have n-doping effect on polymers [38,39].

To solve the air stability issue caused by the high hygroscopic property of PEI, we designed a hydrophobic amine-containing polymer **PDPAT-12** (Fig. 1), which is a copolymer of diphenylamine and thiophene with a dodecyl side group as solubilizing chain on the nitrogen atom of the diphenylamine unit. It was expected that the nitrogen atoms of this polymer would be able to suppress hole transport through a similar mechanism as PEI [34]. **PDPAT-12** was conveniently synthesized *via* the Stille coupling polymerization between *N*-dodecylbis(4-bromophenyl)amine and 5,5′-di-*tert*-butyl-2,2′-bithiophene using a common catalyst system, Pd_2dba_3/P(*o*-tolyl)$_3$ in refluxing toluene. The as-synthesized polymer was purified by Soxhlet extraction with acetone and

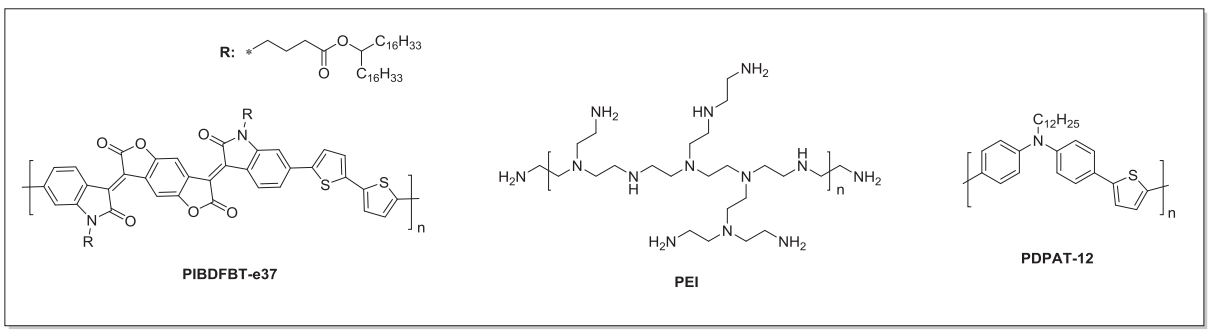

Fig. 1. Chemical structures of ambipolar polymer **PIBDFBT-e37, PEI** (branched polyethylenimine) and amine-containing polymer **PDPAT-12**.

Table 1
Summary of BGBC OTFT performance for pristine **PIBDFBT-e37** or polymer blend films as channel material.[a]

Additive	T_{Ann} (°C)	$\mu_{h,avg}$ (std) ($cm^2\ V^{-1}\ s^{-1}$)	$\mu_{h,max}$ ($cm^2\ V^{-1}\ s^{-1}$)	V_{th} (V)	I_{on}/I_{off}	$\mu_{e,avg}$ (std) ($cm^2\ V^{-1}\ s^{-1}$)	$\mu_{e,max}$ ($cm^2\ V^{-1}\ s^{-1}$)	V_{th} (V)	I_{on}/I_{off}
None	100	0.037 (0.005)	0.044	−60	~10^2	0.21 (0.014)	0.25	15	~10^3
	150	0.036 (0.003)	0.040	−61	~10^2	0.26 (0.015)	0.29	19	~10^3
	200	0.064 (0.009)	0.077	−61	~10^2	0.19 (0.007)	0.21	16	~10^3
2 wt% PEI	100	None				0.25 (0.031)	0.29	13	~10^3
	150	None				0.28 (0.045)	0.34	15	~10^3
	200	None				0.23 (0.042)	0.29	15	~10^3
2 wt% **PDPAT-12**	100	0.0087 (0.0015)	0.012	−55	~10	0.17 (0.0045)	0.18	11	~10^4
	150	0.018 (0.0015)	0.023	−55	~10	0.18 (0.0045)	0.19	14	~10^3
	200	0.044 (0.0032)	0.048	−55	~10	0.22 (0.005)	0.23	18	~10^3
5 wt% **PDPAT-12**	100	1.6×10^{-4} (8×10^{-5})	3.2×10^{-4}	−66		0.25 (0.049)	0.35	38	~10^5
	150	0.0026 (5×10^{-4})	0.0034	−64		0.27 (0.025)	0.33	40	~10^4
	200	0.0048 (0.0013)	0.0068	−64		0.21 (0.013)	0.24	37	~10^4
10 wt% **PDPAT-12**	100	None				0.30 (0.040)	0.42	41	~10^6
	150	3.4×10^{-4} (1×10^{-5})	5.1×10^{-4}	−65		0.26 (0.023)	0.30	36	~10^5
	200	0.0018 (6×10^{-5})	0.0019	−70		0.21 (0.005)	0.22	33	~10^5
20 wt% **PDPAT-12**	100	None				0.061 (0.033)	0.11	42	~10^5
	150	None				0.098 (0.019)	0.12	40	~10^3
	200	None				0.087 (0.022)	0.12	39	~10^3

[a] All devices were tested in dry nitrogen in a glove box and data was obtained from five devices at each condition.

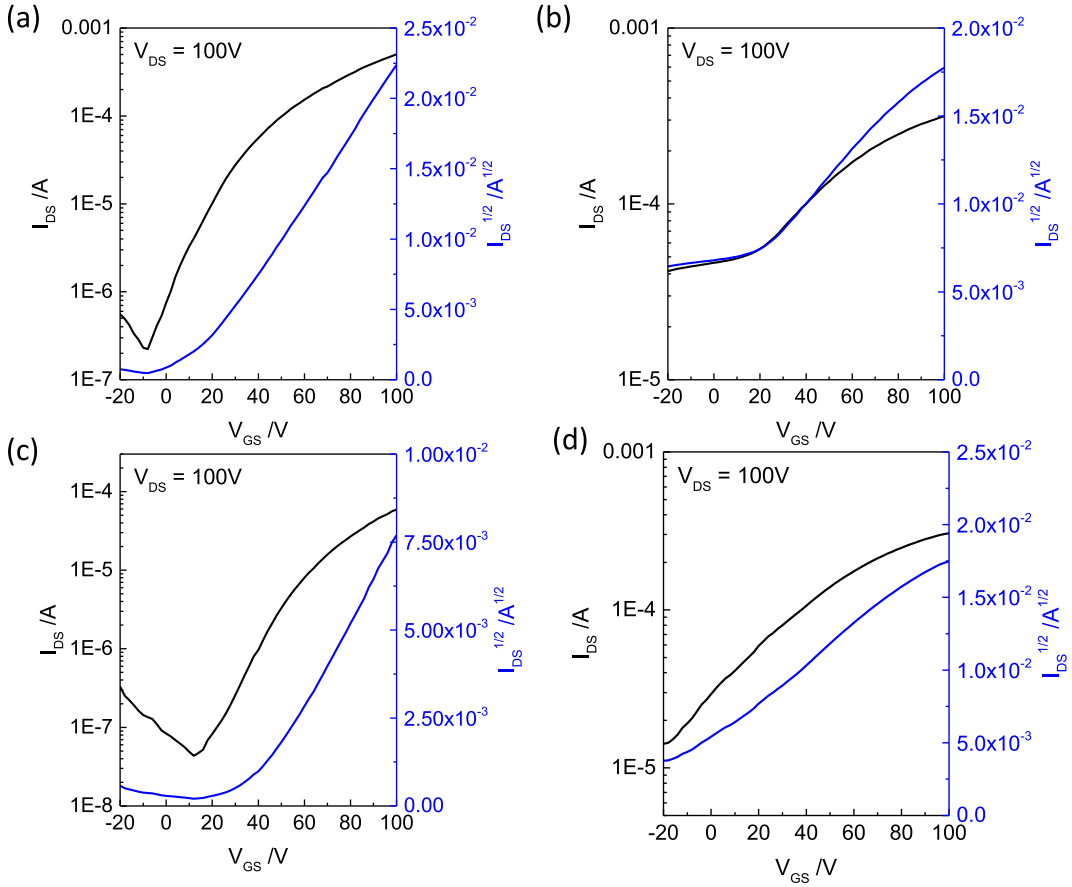

Fig. 2. The transfer curves for 2 wt% PEI in **PIBDFBT-e37** 150 °C-annealed OTFTs tested in dry nitrogen (in a glove box) (a), ambient air (RH = ~50%) (b), dry air (c) and moist nitrogen (d).

hexane and dissolved in chloroform. The polymer has a number average molecular weight (M_n) of 16.2 kDa and a polydispersity index (PDI) of 1.7, which were determined by high temperature-gel permeation chromatography (HT-GPC) (Fig. S3). The thermal stability of this polymer was characterized by thermogravimetric analysis (TGA). The 5% weight loss temperature ($T_{-5\%}$) is 398 °C (Fig. S4), indicating that **PDPAT-12** is thermally very stable. The polymer was also subject to differential scanning calorimetry (DSC) analysis. A glass transition was observed at ~40 °C (Fig. S5) and no melting point was observed, indicating that this polymer is amorphous. The UV–Vis absorption spectra of **PDPAT-12** were measured in both a chloroform solution and thin film (Fig. S6). Based on the absorption onset wavelength, the optical band gap of **PDPAT-12** in solid state was calculated to be 2.62 eV. Cyclic voltammetry was

used to estimate the frontier orbital energy levels of **PDPAT-12** (Fig. S7). Only an oxidation process was observed and the onset potential was used to calculate the HOMO energy level to be −5.27 eV against vacuum (using ferrocene as reference with a HOMO energy of −4.8 eV). The LUMO level is thus estimated to be −2.65 eV by using the optical band gap and the above HOMO energy level. BGBC OTFT devices using **PDPAT-12** as the channel material were fabricated and tested. The devices with **PDPAT-12** films annealed at 100 °C for 20 m showed unipolar hole transport with mobility of ~10^{-4} cm^2 V^{-1} s^{-1} (Fig. S8). Annealing the polymer films at higher temperatures (150 °C and 200 °C) led to lower hole mobilities on the order of 10^{-5} cm^2 V^{-1} s^{-1}. The results indicate that **PDPAT-12** is a poor p-type semiconductor for OTFTs.

To probe the impact of adding **PDPAT-12** on the charge transport properties of **PIBDFBT-e37**, **PIBDFBT-e37**:**PDPAT-12** blends with different weight ratios were prepared and evaluated as channel materials in BGBC OTFTs with the same device configuration used for evaluating the **PIBDFBT-e37**:PEI blends. The **PIBDFBT-e37**:**PDPAT-12** blend films were spin-coated on the substrates and then annealed at 100 °C in a glove box filled with nitrogen. When tested under nitrogen, hole transport in the blend films was suppressed, with hole mobility of 0.0087 cm^2 V^{-1} s^{-1} and 1.6 × 10^{-4} cm^2 V^{-1} s^{-1} for **PIBDFBT-e37**:**PDPAT-12** (2 wt%) and **PIBDFBT-e37**:**PDPAT-12** (5 wt%) blends, respectively (Table 1). This is about two orders of magnitude lower than devices using pristine **PIBDFBT-e37** (Table 1 and Fig. 3), which showed an average hole mobility of up to 0.04 cm^2 V^{-1} s^{-1}. When 10 wt% **PDPAT-12** was added, hole transport was no longer observed (Fig. 3). At the same time, the average electron mobility increased to 0.30 cm^2 V^{-1} s^{-1} (with a maximum value of 0.42 cm^2 V^{-1} s^{-1}) compared to the pristine polymer, which showed average and maximum electron mobilities of 0.21 cm^2 V^{-1} s^{-1} and 0.25 cm^2 V^{-1} s^{-1}, respectively, at the same annealing temperature. The increase in electron mobility most likely resulted from the improved morphology of the blend (see AFM discussion below). Moreover, the on/off current ratio in the n-channel operation was improved to ~10^6, benefiting from the lowered off-current (~10^{-11} A). When the **PDPAT-12** concentration was increased to 20 wt%, the electron mobility dropped to 0.06 cm^2 V^{-1} s^{-1} although it remained unipolar n-type in nature (Table 1). While thermal annealing (Table 1) and air-exposure (Figs. S9 and S10) showed no obvious effect on the threshold voltage (V_{th}) of the OTFT devices with the prisine **PIBDFBT-e37** and the blends, addition of **PDPAT-12** with an amount greater than 5 wt % was found to significantly increase the threshold voltage. We believe the increase in the threshold voltage with addition of **PDPAT-12** is due to the increased electronic defect states at the channel, which trap the injected electrons. It is known that a large threshold voltage may be caused by electronic defect states in the semiconductor, at the interface between semiconductor and dielectric and inside the dielectric layer of an OTFT [40]. Since **PDPAT-12** is amorphous and does not transport electrons, its addition would cause a dilution of **PIBDFBT-e37**, increasing the electronic defect states within the polymer blend and at the interface between the polymer blend and the dielectric layer. Furthermore, the addition of **PDPAT-12** makes the **PIBDFBT-e37** phase more disordered as supported by the XRD data (Fig. 4), which leads to the creation of more electronic defect states in the polymer blend and at the polymer blend and the dielectric interface.

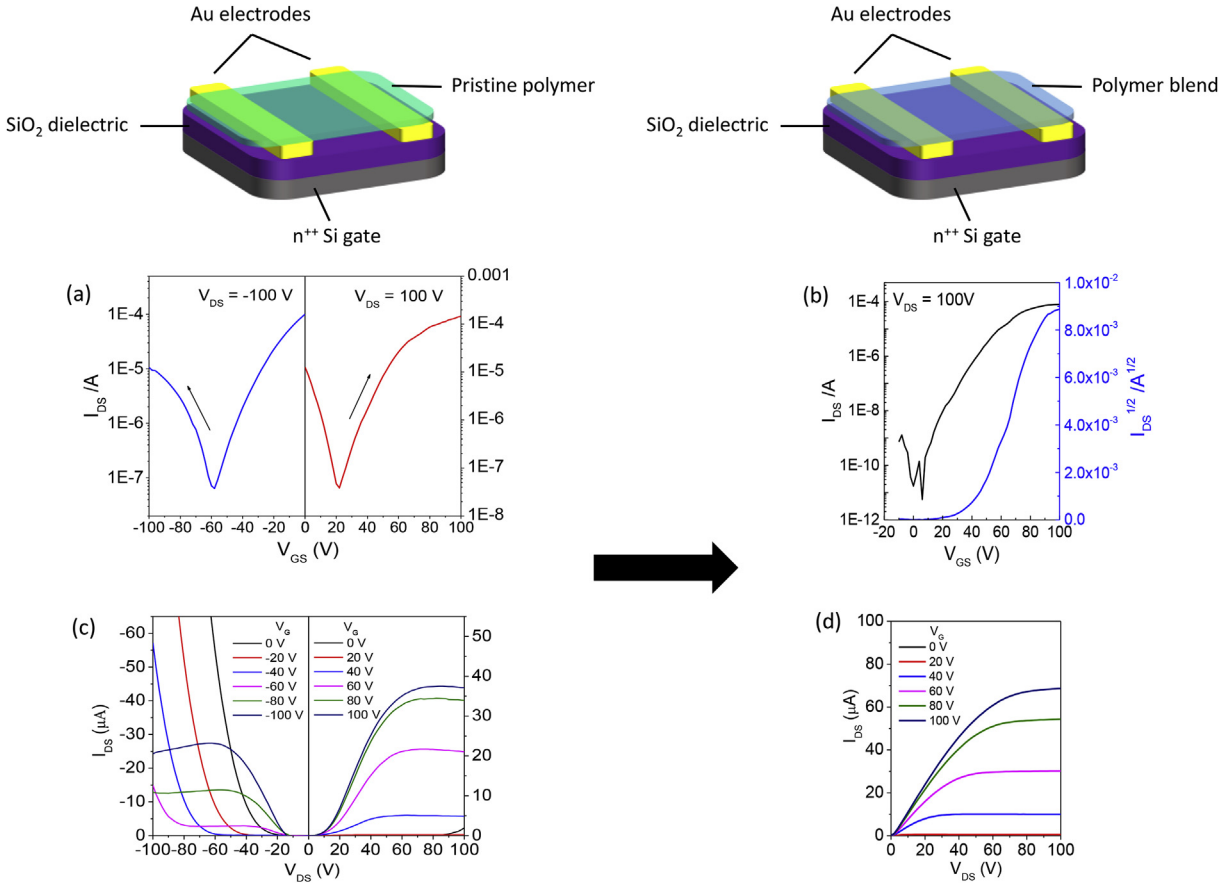

Fig. 3. Output and transfer curves of **PIBDFBT-e37** based OTFTs before (a and c) and after doping with 10 wt% **PDPAT-12** (b and d) tested in dry nitrogen. The polymer films were annealed at 100 °C.

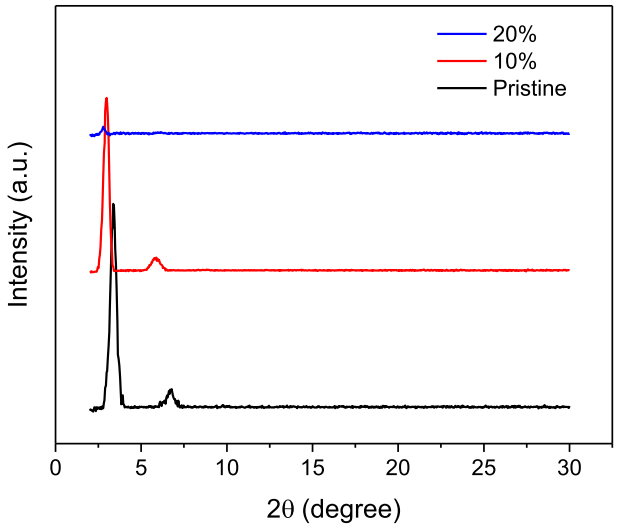

Fig. 4. Out of plane XRD patterns for the pristine **PIBDFBT-e37** film and the **PIBDFBT-e37**:**PDPAT-12** films with different **PDPAT-12** concentrations on SiO_2/Si substrates annealed at 100 °C. The samples were measured in a reflection mode using Cu Kα1 radiation.

In order to verify if polymer chain packing in the blends was disrupted by the presence of **PDPAT-12**, XRD measurements were performed on the polymer films with 0 wt% (pristine), 10 wt% and 20 wt% **PDPAT-12**. The XRD diffraction patterns are shown in Fig. 4. The pristine **PIBDFBT-e37** film showed the primary diffraction peak at $2\theta = 3.36°$ and the secondary diffraction peak at $2\theta = 6.78°$, which corresponds to a *d*-spacing distance of 2.62 nm. This XRD pattern is typical for a polymer film comprising a layer-by-layer lamellar packing motif with predominant edge-on chain packing. The above *d*-spacing represents the interlayer distance separated by the side chains. For the 10 wt% blend film, both the primary and secondary peaks were shifted to smaller angles at $2\theta = 2.97°$ and $2\theta = 5.88°$, respectively, corresponding to a *d*-pacing distance of 2.97 nm. For the 20 wt% blend film, however, the XRD pattern showed poor crystallinity with a very weak primary diffraction peak at $2\theta = 2.78°$ corresponding to a *d*-spacing distance of 3.18 nm. This indicates that the addition of **PDPAT-12** to **PIBDFBT-e37** enlarges the lamellar layer distance and reduces the crystallinity of the polymer semiconductor. It is likely that **PDPAT-12** molecules insert within the lamellar space between the π-π stacked sheets of **PIBDFBT-e37**. When the concentration of **PDPAT-12** reaches 20 wt %, the lamellar layer-by-layer ordering is almost completely disrupted, which is most likely the reason for the poor charge transport property of this blend. AFM measurement was performed to investigate the morphology of the films of **PDPAT-12**, **PIBDFBT-e37** and their blends (with 10 wt% and 20 wt% **PDPAT-12**). As shown in Fig. 5, **PDPAT-12** showed a very smooth morphology with a root mean squared roughness (RMS) of 0.57 nm, while **PIBDFBT-e37** showed a much rougher morphology with a RMS of 5.3 nm. With 10 wt% **PDPAT-12** in **PIBDFBT-e37**, the RMS of the blend film decreased to 2.6 nm. In addtion, in the 10 wt% **PDPAT-12** blend film, the grains are well connected to form a more continuous network in comparison with the pristine **PIBDFBT-e37** that is composed of much larger and isolated grains. The continuous network formed within the 10 wt% **PDPAT-12** blend film might contribute to its improved electron mobility in OTFTs. With 20 wt% **PDPAT-12**, the film became quite amorphous, which is supported by the XRD study (Fig. 4), leading to a drop in the electron mobility (Table 1). To probe the hole trapping mechanism, we performed UV–Vis–NIR absorption spectroscopy on the as-spun films of pristine **PIBDFBT-e37**, **PIBDFBT-e37**:**PDPAT-12** (10 wt%) and **PIBDFBT-e37**:**PDPAT-12** (20 wt%) (Fig. S11). The **PIBDFBT-e37:PDPAT-12** films showed almost no changes in the absorption region (~500–1000 nm) that represent **PIBDFBT-e37**, which indicates that there was no charge transfer between **PDPAT-12** and **PIBDFBT**. On one hand, the hole trapping can be due to the electron lone pairs on the nitrogen atoms in **PDPAT-12**, similar to the hole trapping mechanism proposed for PEI [34]. On the other hand, it might be due to the rather high HOMO energy level (−5.27 eV) of **PDPAT-12** with respect to that of **PIBDFBT-e37** (−5.72 eV) [11]. Recently, we found that addition of a small molecule aromatic amine with a HOMO energy level ~0.25 eV higher than that of the host polymer could effectively suppress hole transport of an ambipolar polymer and convert it into n-type polymer [41]. The HOMO energy difference between the small aromatic amine and the host polymer is termed the trap energy, E_T. By comparing the HOMO energies of **PDPAT-12** and **PIBDFBT-e37** (Fig. 6), the E_T is estimated to be 0.45 eV, which is sufficient for trapping the injected holes at the HOMO of **PDPAT-12**.

Finally, we evaluated the performance of BGBC OTFT devices with the **PIBDFBT-e37**:**PDPAT-12** (10 wt%) blend along with those of devices based on the pristine **PIBDFBT-e37** in the ambient air (RH = ~50%). All devices were annealed at 100 °C for 20 min. The devices were stored and tested in ambient air over a period of 28 days (Fig. 7). In the initial testing, the polymer blend-based devices were able to achieve unipolar n-type charge transport with average electron mobility of 0.16 $cm^2\ V^{-1}\ s^{-1}$ (with a maximum value of 0.19 $cm^2\ V^{-1}\ s^{-1}$), while the pristine polymer-based devices showed ambipolar charge transport with average electron mobility of 0.14 $cm^2\ V^{-1}\ s^{-1}$ (with a maximum value of 0.18 $cm^2\ V^{-1}\ s^{-1}$) and an average hole mobility of 0.012 $cm^2\ V^{-1}\ s^{-1}$ (with a maximum value of 0.013 $cm^2\ V^{-1}\ s^{-1}$). After exposure to ambient air for 28 days, the average electron mobilities of the polymer blend and pristine polymer dropped to 0.08 $cm^2\ V^{-1}\ s^{-1}$ (50% of the initial value) and 0.018 $cm^2\ V^{-1}\ s^{-1}$ (13% of the initial value), respectively, showing that the polymer blend is more robust in ambient air than the pristine polymer. The LUMO energy of **PIBDFBT-e37** is −3.87 eV, which is close to the borderline of the LUMO energy of ca. −4.0 eV [42–46] that is required for stable n-channel operation of an OTFTs in the presence of oxygen and moisture in ambient air. This explains the fact that **PIBDFBT-e37** showed degradation of electron transport in air over time (Fig. 7). To investigate the effect of the added **PDPAT-12** on the moisture resistance of the blend films, we measured the water contact angles of the pristine **PIBDFBT-e37** and the **PIBDFBT-e37**:**PDPAT-12** (10 wt%) blend films. They showed very similar water contact angles of 123.6° for **PIBDFBT-e37** and 121.4° for the **PIBDFBT-e37**:**PDPAT-12** blend (10 wt%) (Fig. S12), indicating that the moisture resistance of the blend films was almost not changed with the addtion of **PDPAT-12**. Previous studies showed that electron-rich aromatic amine compounds can serve as oxygen scavengers to inhibit oxidation of polymer materials [47–49]. Therefore, it is reasonable to consider that the aromatic amine polymer **PDPAT-12** may interact with oxygen diffused into the active layer more preferentially compared to **PIBDFBT-e37**, leading to the improved air stability of OTFTs with the polymer blends.

3. Methods

3.1. Materials and characterization

All chemicals were obtained from commercial sources and used as received. *N*-dodecylbis(4-bromophenyl)amine [50] and **PIBDFBT-e37** [11] were prepared according to the literature methods. High-temperature gel permeation chromatography (HT-GPC) measurements were performed on a Malvern 350 HT-GPC

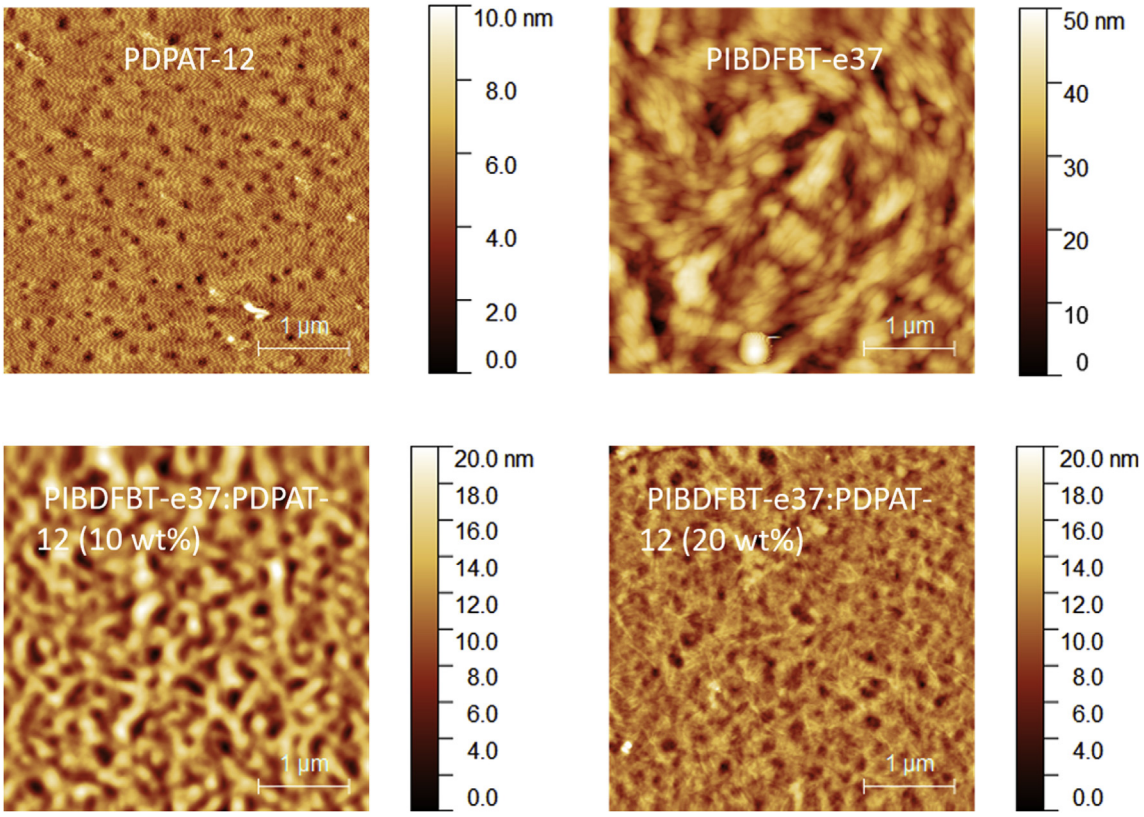

Fig. 5. AFM images for the films of pristine **PDPAT-12**, **PIBDFBT-e37** and theirs blends spin coated on dodecyltrichlorosilane (DDTS)-modified SiO_2/Si substrates and annealed at 100 °C.

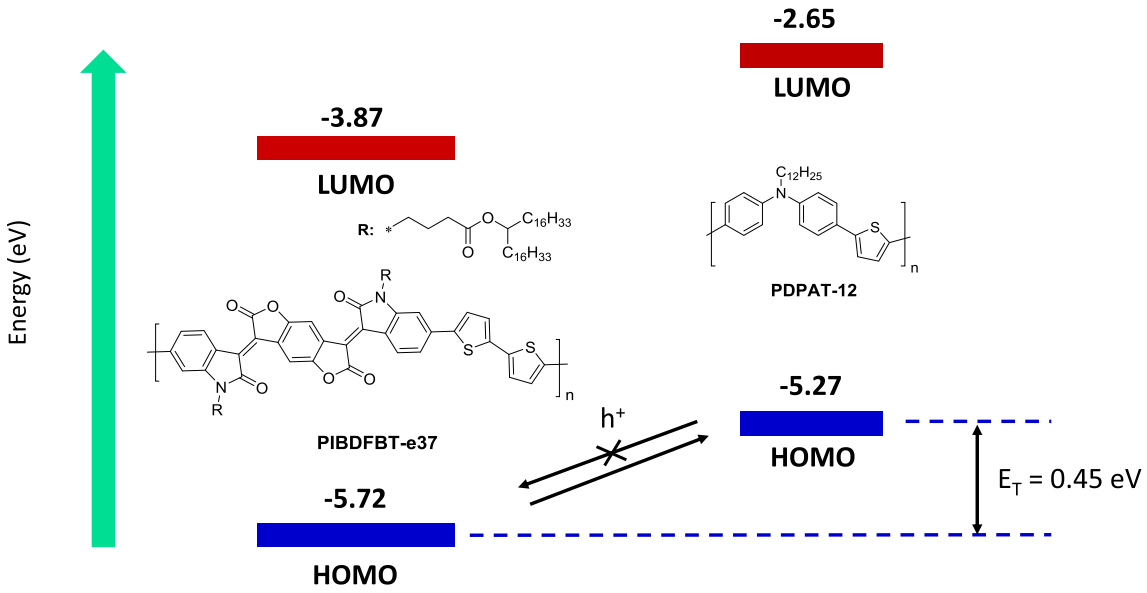

Fig. 6. The frontier energies of **PIBDFBT-e37** and **PDPAT-12** and the hole trapping effect of **PDPAT-12** due to its much higher HOMO energy level than that of **PIBDFBT-e37**, creating a large trap energy (E_T) of 0.45 eV.

system using 1,2,4-trichlorobenzene as eluent and polystyrene as standards at a column temperature of 140 °C. Thermogravimetric analysis (TGA) was carried out on a TA Instruments SDT 2960 at a scan rate of 10 °C min^{-1} under nitrogen. Differential scanning calorimetry (DSC) was carried out on a TA Instruments Q2000 at a temperature ramping rate of 20 °C min^{-1} under nitrogen. The UV–Vis absorption spectra of the polymer were recorded on a Thermo Scientific model GENESYS™ 10S VIS spectrophotometer. Cyclic voltammetry (CV) data was collected on a CHI600E electrochemical analyser using an Ag/AgCl reference electrode and two Pt disk electrodes as the working and counter electrodes in a 0.1 M tetrabutylammonium hexafluorophosphate solution in acetonitrile

at a scan rate of 50 mV s^{-1}. Ferrocene was used as the reference, which has a HOMO energy value of −4.8 eV [51]. The nuclear magnetic resonance (NMR) spectrum was obtained with a Bruker DPX 300 MHz spectrometer with chemical shifts relative to tetramethylsilane (TMS, 0 ppm). Reflective X-ray diffraction measurements were carried out on a Bruker D8 Advance diffractometer with Cu Kα1 radiation (λ = 0.15406 nm) using polymer films spin-coated on SiO_2/Si substrates.

3.2. Fabrication and characterization of OTFT devices

The bottom-contact bottom-gate (BGBC) configuration was adopted for all OTFT devices. The preparation procedure of the substrate and device is as follows. A heavily n-doped Si wafer with ~300 nm-thick SiO_2 layer was patterned with gold source and drain pairs by conventional photolithography and the subsequent thermal deposition of gold. Then the substrate was treated with air plasma, followed by cleaning with acetone and isopropanol in an ultrasonic bath. Subsequently, the substrate surface was modified by merging in a 3% dodecyltrichlorosilane (DDTS) solution in toluene at room temperature for 20 min. The modified substrate was washed with toluene and dried under a nitrogen flow. Then the **PIBDFBT-e37** film was spin-coated onto the substrate at 3000 rpm for 60 s using a **PIBDFBT-e37** solution in chloroform (5 mg mL^{-1}) in a nitrogen-filled glove box. For spin-coating the polymer blend films, PEI (branched polyethylenimine with an M_w of ~25,000 by light scattering and an M_n of 10,000 by GPC, purchased from Sigma Aldrich) or **PDPAT-12** was added to **PIBDFBT-e37** and then the mixture was dissolved in chloroform to form a polymer solution with a total concentration of 5 mg mL^{-1}. After spin-coating, the obtained film was subject to thermal annealing at a certain temperature for 20 min in a glove box. Then the devices were characterized in dry nitrogen (inside the glove box), ambient air, dry air or moist nitrogen using an Agilent B2912A semiconductor analyser. The hole and electron mobilities are calculated in the saturation regime according to the following equation:

$$I_{DS} = \frac{\mu C_i W}{2L}(V_{GS} - V_{th})^2$$

where I_{DS} is the drain-source current, μ is charge carrier mobility, C_i is the gate dielectric layer capacitance per unit area (~11.6 nF cm^{-2}), V_{GS} is the gate voltage, V_{th} is the threshold voltage, L is the channel length (30 μm), and W is the channel width (1000 μm).

3.3. Synthesis of PDPAT-12

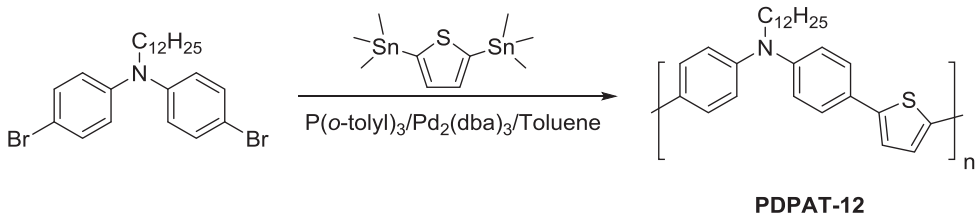

PDPAT-12

To a Schlenk flask N-dodecylbis(4-bromophenyl)amine (182 mg, 0.367 mmol), 2,5-bis(trimethylstannyl)thiophene (160 mg, 0.367 mmol), tri(*o*-tolyl)phosphine P(*o*-tol)$_3$ (9.1 mg, 29.4 μmol), tris(dibenzylideneacetone)dipalladium (Pd_2dba_3) (6.7 mg, 7.34 μmol) and toluene (10 mL) and were added under argon. The mixture was stirred under reflux for 48 h. Afterwards the reaction mixture was poured into methanol under stirring. The precipitated solid was collected by filtration and then subject to Soxhlet extraction with acetone, hexane and chloroform sequentially. The title polymer was obtained by drying the chloroform fraction. Yield: 70.2 mg (48%). HT-GPC (140 °C) data: M_n = 16.2 kDa and PDI = 1.7 (against polystyrene standards).

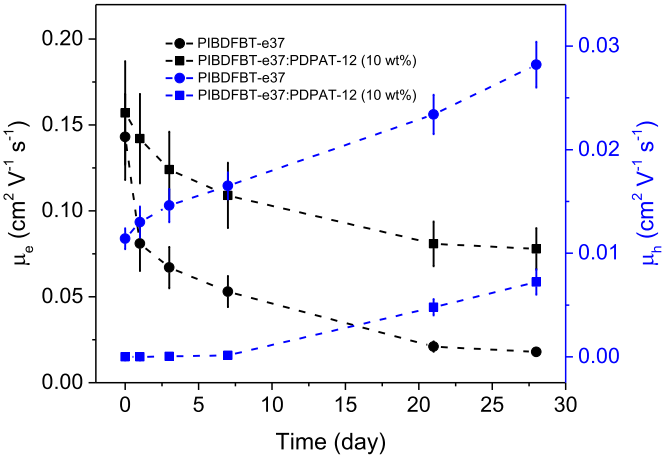

Fig. 7. The electron and hole mobilities of BGBC OTFTs with 100 °C-annealed pristine **PIBDFBT-e37** and **PIBDFBT-e37**:**PDPAT-12** (10 wt%) blend films over 28 days. All devices were stored and tested in ambient air (RH = ~50%).

4. Conclusion

It was found in this study that PEI as an additive could covert the ambipolar polymer **PIBDFBT-e37** into a unipolar n-type polymer in BGBC OTFTs when the devices were measured in dry nitrogen. However, the devices measured in ambient air (RH = ~50%) showed severely degraded transistor performance and significantly increased off current, which was proven to be due to the interaction of the polymer blend with the moisture in ambient air. To overcome the moisture sensitivity issue of PEI, a hydrophobic aromatic amine polymer, **PDPAT-12**, was synthesized and used to convert **PIBDFBT-e37** into a unipolar n-type polymer. With 10 wt% **PDPAT-12** addition, the polymer blend exhibited unipolar n-type charge transport characteristic with electron mobilities of up to 0.42 cm^2 V^{-1} s^{-1} in dry nitrogen and 0.19 cm^2 V^{-1} s^{-1} in ambient air. The observed hole suppression effect of **PDPAT-12** is considered due to the hole trapping by the electron lone pairs of the nitrogen atoms in **PDPAT-12** as well as the large trap energy of this polymer with respect to the host polymer **PIBDFBT-e37**. The BGBC OTFTs with a **PIBDFBT-e37: PDPAT-12** (10 wt%) blend were able to maintain 50% of their initial electron mobility after exposure to ambient air (RH = ~50%) for 28 days. In comparison, the pristine **PIBDFBT-e37** could only

keep 13% of its initial electron mobility under the same conditions. Our study shows that this aromatic amine polymer, **PDPAT-12**, is very useful in converting ambipolar polymers into unipolar n-type polymers with improved electron mobility and stability in ambient air.

Acknowledgements

The authors thank the Natural Sciences and Engineering Research Council (NSERC) of Canada for financial support of this work (Discovery Grants # RGPIN-2016-04366).

Appendix A. Supplementary data

Supplementary data related to this article can be found at http://dx.doi.org/10.1016/j.orgel.2017.07.016.

References

[1] A.J. Heeger, Semiconducting polymers: the third generation, Chem. Soc. Rev. 39 (2010) 2354–2371, http://dx.doi.org/10.1039/B914956M.
[2] C. Wang, H. Dong, W. Hu, Y. Liu, D. Zhu, Semiconducting π-conjugated systems in field-effect transistors: a material odyssey of organic electronics, Chem. Rev. 112 (2012) 2208–2267, http://dx.doi.org/10.1021/cr100380z.
[3] A.C. Arias, J.D. MacKenzie, I. McCulloch, J. Rivnay, A. Salleo, Materials and applications for large area electronics: solution-based approaches, Chem. Rev. 110 (2010) 3–24, http://dx.doi.org/10.1021/cr900150b.
[4] A. Zhang, C. Xiao, Y. Wu, C. Li, Y. Ji, L. Li, W. Hu, Z. Wang, W. Ma, W. Li, Effect of fluorination on molecular orientation of conjugated polymers in high performance field-effect transistors, Macromolecules 49 (2016) 6431–6438, http://dx.doi.org/10.1021/acs.macromol.6b01446.
[5] G. Kim, S.-J. Kang, G.K. Dutta, Y.-K. Han, T.J. Shin, Y.-Y. Noh, C. Yang, A thienoisoindigo-naphthalene polymer with ultrahigh mobility of 14.4 $cm^2/V{\cdot}s$ that substantially exceeds benchmark values for amorphous silicon semiconductors, J. Am. Chem. Soc. 136 (2014) 9477–9483, http://dx.doi.org/10.1021/ja504537v.
[6] B. Sun, W. Hong, Z. Yan, H. Aziz, Y. Li, Record high electron mobility of 6.3 $cm^2V^{-1}s^{-1}$ achieved for polymer semiconductors using a new building block, Adv. Mater. 26 (2014) 2636–2642, http://dx.doi.org/10.1002/adma.201305981.
[7] I. Kang, H.-J. Yun, D.S. Chung, S.-K. Kwon, Y.-H. Kim, Record high hole mobility in polymer semiconductors via side-chain engineering, J. Am. Chem. Soc. 135 (2013) 14896–14899, http://dx.doi.org/10.1021/ja405112s.
[8] H.-J. Yun, S.-J. Kang, Y. Xu, S.O. Kim, Y.-H. Kim, Y.-Y. Noh, S.-K. Kwon, Organic field-effect transistors: dramatic inversion of charge polarity in diketopyrrolopyrrole-based organic field-effect transistors via a simple nitrile group substitution, Adv. Mater. 26 (2014) 7282, http://dx.doi.org/10.1002/adma.201470294.
[9] H. Sirringhaus, 25th anniversary article: organic field-effect transistors: the path beyond amorphous silicon, Adv. Mater. 26 (2014) 1319–1335, http://dx.doi.org/10.1002/adma.201304346.
[10] J. Lee, A.-R. Han, H. Yu, T.J. Shin, C. Yang, J.H. Oh, Boosting the ambipolar performance of solution-processable polymer semiconductors via hybrid side-chain engineering, J. Am. Chem. Soc. 135 (2013) 9540–9547, http://dx.doi.org/10.1021/ja403949g.
[11] Y. He, C. Guo, B. Sun, J. Quinn, Y. Li, Branched alkyl ester side chains rendering large polycyclic (3E,7E)-3,7-bis(2-oxoindolin-3-ylidene)benzo[1,2-b:4,5-b[prime or minute]]difuran-2,6(3H,7H)-dione (IBDF) based donor-acceptor polymers solution-processability for organic thin film transistors, Polym. Chem. 6 (2015) 6689–6697, http://dx.doi.org/10.1039/C5PY00782H.
[12] W. Hong, B. Sun, C. Guo, J. Yuen, Y. Li, S. Lu, C. Huang, A. Facchetti, Dipyrrolo[2,3-b:2′,3′-e]pyrazine-2,6(1H,5H)-dione based conjugated polymers for ambipolar organic thin-film transistors, Chem. Commun. 49 (2013) 484–486, http://dx.doi.org/10.1039/C2CC37266E.
[13] Z. Yan, B. Sun, Y. Li, Novel stable (3E,7E)-3,7-bis(2-oxoindolin-3-ylidene)benzo[1,2-b:4,5-b[prime or minute]]difuran-2,6(3H,7H)-dione based donor-acceptor polymer semiconductors for n-type organic thin film transistors, Chem. Commun. 49 (2013) 3790–3792, http://dx.doi.org/10.1039/C3CC40531A.
[14] W. Hong, C. Guo, B. Sun, Y. Li, (3Z,3′Z)-3,3′-(Hydrazine-1,2-diylidene)bis(indolin-2-one) as a new electron-acceptor building block for donor-acceptor [small pi]-conjugated polymers for organic thin film transistors, J. Mater. Chem. C 3 (2015) 4464–4470, http://dx.doi.org/10.1039/C5TC00447K.
[15] Y. He, C. Guo, B. Sun, J. Quinn, Y. Li, (3E,7E)-3,7-Bis(2-oxoindolin-3-ylidene)-5,7-dihydropyrrolo[2,3-f]indole-2,6(1H,3H)-dione based polymers for ambipolar organic thin film transistors, Chem. Commun. 51 (2015) 8093–8096, http://dx.doi.org/10.1039/C5CC01021G.
[16] Y. He, J. Quinn, Y. Deng, Y. Li, 3,7-Bis((E)-2-oxoindolin-3-ylidene)-3,7-dihydrobenzo[1,2-b:4,5-b′]dithiophene-2,6-dione (IBDT) based polymer with balanced ambipolar charge transport performance, Org. Electron. 35 (2016) 41–46, http://dx.doi.org/10.1016/j.orgel.2016.05.003.
[17] M. Bronner, A. Opitz, W. Brütting, Ambipolar charge carrier transport in organic semiconductor blends of phthalocyanine and fullerene, Phys. Status Solidi 205 (2008) 549–563, http://dx.doi.org/10.1002/pssa.200723405.
[18] J. Quinn, H. Patel, F. Haider, D.A. Khan, Y. Li, Converting a semiconducting polymer from ambipolar into n-type dominant by amine end-capping, ChemElectroChem 4 (2017) 256–260, http://dx.doi.org/10.1002/celc.201600628.
[19] Y. Li, P. Sonar, S.P. Singh, M.S. Soh, M. Van Meurs, J. Tan, Annealing-free high-mobility diketopyrrolopyrrole-quaterthiophene copolymer for solution-processed organic thin film transistors, J. Am. Chem. Soc. 133 (2011) 2198–2204, http://dx.doi.org/10.1021/ja1085996.
[20] T. Lei, J.H. Dou, J. Pei, Influence of alkyl chain branching positions on the hole mobilities of polymer thin-film transistors, Adv. Mater. 24 (2012) 6457–6461, http://dx.doi.org/10.1002/adma.201202689.
[21] I. Kang, T.K. An, J. Hong, H.-J. Yun, R. Kim, D.S. Chung, C.E. Park, Y.-H. Kim, S.-K. Kwon, Effect of selenophene in a DPP copolymer incorporating a vinyl group for high-performance organic field-effect transistors, Adv. Mater. 25 (2013) 524–528, http://dx.doi.org/10.1002/adma.201202867.
[22] S. Chen, B. Sun, W. Hong, H. Aziz, Y. Meng, Y. Li, Influence of side chain length and bifurcation point on the crystalline structure and charge transport of diketopyrrolopyrrole-quaterthiophene copolymers (PDQTs), J. Mater. Chem. C 2 (2014) 2183–2190, http://dx.doi.org/10.1039/c3tc32219j.
[23] J. Choi, H. Song, N. Kim, F.S. Kim, Development of n-type polymer semiconductors for organic field-effect transistors, Semicond. Sci. Technol. 30 (2015) 64002, http://dx.doi.org/10.1088/0268-1242/30/6/064002.
[24] Y.-Z. Dai, N. Ai, Y. Lu, Y.-Q. Zheng, J.-H. Dou, K. Shi, T. Lei, J.-Y. Wang, J. Pei, Embedding electron-deficient nitrogen atoms in polymer backbone towards high performance n-type polymer field-effect transistors, Chem. Sci. 7 (2016) 5753–5757, http://dx.doi.org/10.1039/C6SC01380E.
[25] Y. Deng, B. Sun, Y. He, J. Quinn, C. Guo, Y. Li, Thiophene-S,S-dioxidized indophenine: a quinoid-type building block with high electron affinity for constructing n-type polymer semiconductors with narrow band gaps, Angew. Chem. Int. Ed. 55 (2016) 3459–3462, http://dx.doi.org/10.1002/anie.201508781.
[26] T. Lei, J.-H. Dou, X.-Y. Cao, J.-Y. Wang, J. Pei, A BDOPV-based donor-acceptor polymer for high-performance n-type and oxygen-doped ambipolar field-effect transistors, Adv. Mater. 25 (2013) 6589–6593, http://dx.doi.org/10.1002/adma.201302278.
[27] T. Lei, J.-H. Dou, X.-Y. Cao, J.-Y. Wang, J. Pei, Electron-Deficient poly(p-phenylene vinylene) provides electron mobility over 1 $cm^2V^{-1}s^{-1}$ under ambient conditions, J. Am. Chem. Soc. 135 (2013) 12168–12171, http://dx.doi.org/10.1021/ja403624a.
[28] T. Lei, X. Xia, J.-Y. Wang, C.-J. Liu, J. Pei, "Conformation locked" strong electron-deficient poly(p-phenylene vinylene) derivatives for ambient-stable n-type field-effect transistors: synthesis, properties, and effects of fluorine substitution position, J. Am. Chem. Soc. 136 (2014) 2135–2141, http://dx.doi.org/10.1021/ja412533d.
[29] J.-H. Dou, Y.-Q. Zheng, T. Lei, S.-D. Zhang, Z. Wang, W.-B. Zhang, J.-Y. Wang, J. Pei, Systematic investigation of side-chain branching position effect on electron carrier mobility in conjugated polymers, Adv. Funct. Mater. 24 (2014) 6270–6278, http://dx.doi.org/10.1002/adfm.201401822.
[30] Y.-Q. Zheng, T. Lei, J.-H. Dou, X. Xia, J.-Y. Wang, C.-J. Liu, J. Pei, Strong electron-deficient polymers lead to high electron mobility in air and their morphology-dependent transport behaviors, Adv. Mater. 28 (2016) 7213–7219, http://dx.doi.org/10.1002/adma.201600541.
[31] G. Zhang, P. Li, L. Tang, J. Ma, X. Wang, H. Lu, B. Kang, K. Cho, L. Qiu, A bis(2-oxoindolin-3-ylidene)-benzodifuran-dione containing copolymer for high-mobility ambipolar transistors, Chem. Commun. 50 (2014) 3180, http://dx.doi.org/10.1039/c3cc48695h.
[32] G. Zhang, J. Guo, M. Zhu, P. Li, H. Lu, K. Cho, L. Qiu, Bis(2-oxoindolin-3-ylidene)-benzodifuran-dione-based D-A polymers for high-performance n-channel transistors, Polym. Chem. 6 (2015) 2531–2540, http://dx.doi.org/10.1039/C4PY01683A.
[33] X. Wang, H.H. Choi, G. Zhang, Y. Ding, H. Lu, K. Cho, L. Qiu, Bis(2-oxoindolin-3-ylidene)-benzodifuran-dione and bithiophene-based conjugated polymers for high performance ambipolar organic thin-film transistors: the impact of substitution positions on bithiophene units, J. Mater. Chem. C 4 (2016) 6391–6400, http://dx.doi.org/10.1039/C6TC01617K.
[34] B. Sun, W. Hong, E.S. Thibau, H. Aziz, Z.-H. Lu, Y. Li, Polyethylenimine (PEI) as an effective dopant to conveniently convert ambipolar and p-type polymers into unipolar n-type polymers, ACS Appl. Mater. Interfaces 7 (2015) 18662–18671, http://dx.doi.org/10.1021/acsami.5b05097.
[35] X. Zhou, N. Ai, Z.-H. Guo, F.-D. Zhuang, Y.-S. Jiang, J.-Y. Wang, J. Pei, Balanced ambipolar organic thin-film transistors operated under ambient conditions: role of the donor moiety in BDOPV-based conjugated copolymers, Chem. Mater. 27 (2015) 1815–1820, http://dx.doi.org/10.1021/acs.chemmater.5b00018.
[36] H.T. Nicolai, M. Kuik, G.A.H. Wetzelaer, B. de Boer, C. Campbell, C. Risko, J.L. Brédas, P.W.M. Blom, Unification of trap-limited electron transport in semiconducting polymers, Nat. Mater. 11 (2012) 882–887, http://dx.doi.org/10.1038/nmat3384.
[37] A. von Harpe, H. Petersen, Y. Li, T. Kissel, Characterization of commercially available and synthesized polyethylenimines for gene delivery, J. Control.

Release 69 (2000) 309–322, http://dx.doi.org/10.1016/S0168-3659(00)00317-5.
[38] D. Henkensmeier, H.-J. Kim, H.-J. Lee, D.H. Lee, I.-H. Oh, S.-A. Hong, S.-W. Nam, T.-H. Lim, Polybenzimidazolium-based solid electrolytes, Macromol. Mater. Eng. 296 (2011) 899–908, http://dx.doi.org/10.1002/mame.201100100.
[39] O.D. Thomas, K.J.W.Y. Soo, T.J. Peckham, M.P. Kulkarni, S. Holdcroft, A stable hydroxide-conducting polymer, J. Am. Chem. Soc. 134 (2012) 10753–10756, http://dx.doi.org/10.1021/ja303067t.
[40] H. Sirringhaus, Device physics of solution-processed organic field-effect transistors, Adv. Mater. 17 (2005) 2411–2425, http://dx.doi.org/10.1002/adma.200501152.
[41] B. Sun, W. Hong, C. Guo, S. Sutty, H. Aziz, Y. Li, Utilization of hole trapping effect of aromatic amines to convert polymer semiconductor from ambipolar into n-type, Org. Electron. 37 (2016) 190–196, http://dx.doi.org/10.1016/j.orgel.2016.06.028.
[42] J. Zaumseil, H. Sirringhaus, Electron and ambipolar transport in organic field-effect transistors, Chem. Rev. 107 (2007) 1296–1323, http://dx.doi.org/10.1021/cr0501543.
[43] B.A. Jones, M.J. Ahrens, M.-H. Yoon, A. Facchetti, T.J. Marks, M.R. Wasielewski, High-Mobility Air-Stable n-Type Semiconductors with Processing Versatility: dicyanoperylene-3,4:9,10-bis(dicarboximides), Angew. Chem. Int. Ed. 43 (2004) 6363–6366, http://dx.doi.org/10.1002/anie.200461324.
[44] H.E. Katz, A.J. Lovinger, J. Johnson, C. Kloc, T. Siegrist, W. Li, Y.-Y. Lin, A. Dodabalapur, A soluble and air-stable organic semiconductor with high electron mobility, Nature 404 (2000) 478–481, http://dx.doi.org/10.1038/35006603.
[45] Z.F. Li, E.T. Kang, K.G. Neoh, K.L. Tan, Effect of thermal processing conditions on the intrinsic oxidation states and mechanical properties of polyaniline films, Synth. Met. 87 (1997) 45–52, http://dx.doi.org/10.1016/S0379-6779(97)80096-3.
[46] B.A. Jones, A. Facchetti, M.R. Wasielewski, T.J. Marks, Tuning orbital energetics in arylene diimide semiconductors. Materials design for ambient stability of n-type charge transport, J. Am. Chem. Soc. 129 (2007) 15259–15278, http://dx.doi.org/10.1021/ja075242e.
[47] C.E. Hoyle, K.-J. Kim, The effect of aromatic amines on the photo-polymerization of 1,6-hexanediol diacrylate, J. Appl. Polym. Sci. 33 (1987) 2985–2996, http://dx.doi.org/10.1002/app.1987.070330831.
[48] C. Decker, A.D. Jenkins, Kinetic approach of oxygen inhibition in ultraviolet- and laser-induced polymerizations, Macromolecules 18 (1985) 1241–1244, http://dx.doi.org/10.1021/ma00148a034.
[49] D.L. Zabrowski, A.E. Moormann, K.R. Beck, The oxidation of aromatic amines in the presence of?electron-rich? aromatic systems, Tetrahedron Lett. 29 (1988) 4501–4504, http://dx.doi.org/10.1016/S0040-4039(00)80531-6.
[50] K. Idzik, J. Sołoducho, J. Cabaj, M. Mosiądz, M. Łapkowski, S. Golba, Novel aspects of a convenient synthesis and of electroproperties of derivatives based on diphenylamine, Helv. Chim. Acta 91 (2008) 618–627, http://dx.doi.org/10.1002/hlca.200890065.
[51] J. Pommerehne, H. Vestweber, W. Guss, R.F. Mahrt, H. Bassler, M. Porsch, J. Daub, Efficient two layer leds on a polymer blend basis, Adv. Mater. 7 (1995) 551–554, http://dx.doi.org/10.1002/adma.19950070608.